

# Training-free Motion Factorization for Compositional Video Generation

Zixuan Wang  
Sichuan University  
Chengdu, China

zixuan98@stu.scu.edu.cn

Ziqin Zhou  
The University of Adelaide  
Adelaide, Australia

ziqin.zhou@adelaide.edu.au

Feng Chen  
The University of Adelaide  
Adelaide, Australia

chenfeng1271@gmail.com

Duo Peng  
Singapore University of Technology and Design  
Singapore

duo\_peng@mymail.sutd.edu.sg

Yixin Hu  
Sichuan University  
Chengdu, China

yixinhu@stu.scu.edu.cn

Changsheng Li  
Beijing Institute of Technology  
Beijing, China

lcs@bit.edu.cn

Yinjie Lei†  
Sichuan University  
Chengdu, China

yinjie@scu.edu.cn

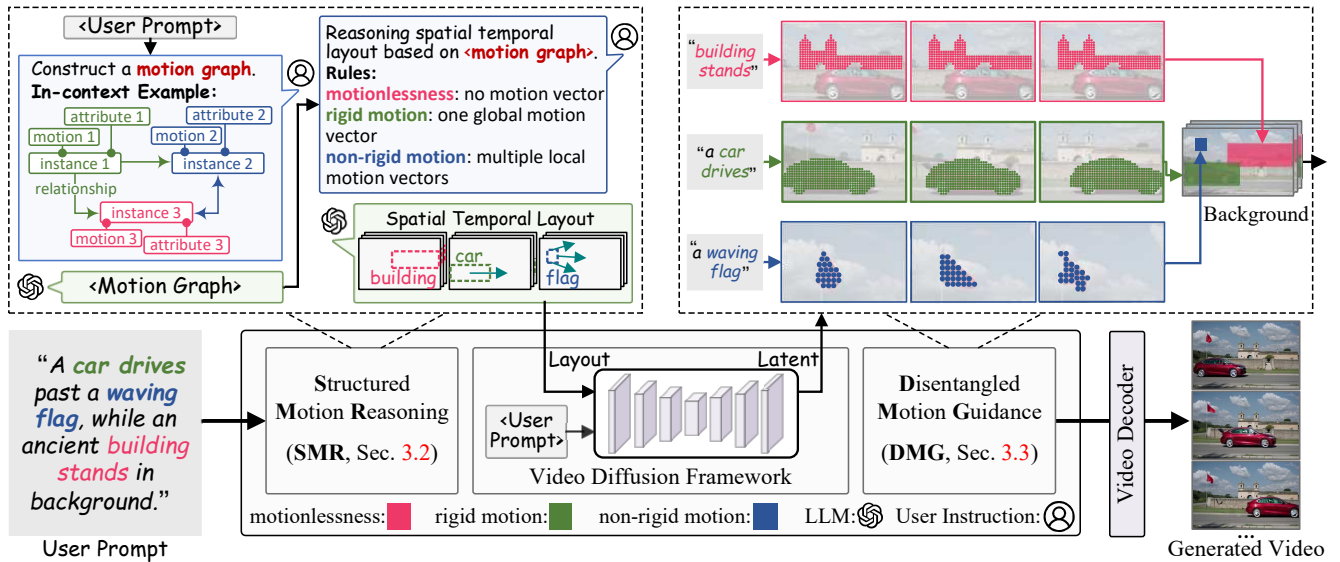


Figure 1. Overview of our motion factorization framework. First, for each instance belonging to a particular motion category, our framework infers its per-frame changes in shape and position from a structured motion graph (Sec. 3.2). Second, conditioned on the motion category, dedicated guidance branches synthesize per-instance motions, which are subsequently composed into a coherent scene (Sec. 3.3).

## Abstract

Compositional video generation aims to synthesize multiple instances with diverse appearance and motion, which is widely applicable in real-world scenarios. However, current approaches mainly focus on binding semantics, neglecting to understand diverse motion categories specified

† Corresponding author.

in prompts. In this paper, we propose a **motion factorization** framework that decomposes complex motion into three primary categories: motionlessness, rigid motion, and non-rigid motion. Specifically, our framework follows a planning before generation paradigm. (1) During planning, we reason about motion laws on the motion graph to obtain frame-wise changes in the shape and position of each instance. This alleviates semantic ambiguities in the user

*prompt by organizing it into a structured representation of instances and their interactions. (2) During generation, we modulate the synthesis of distinct motion categories in a disentangled manner. Conditioned on the motion cues, guidance branches stabilize appearance in motionless regions, preserve rigid-body geometry, and regularize local non-rigid deformations. Crucially, our two modules are model-agnostic, which can be seamlessly incorporated into various diffusion model architectures. Extensive experiments demonstrate that our framework achieves impressive performance in motion synthesis on real-world benchmarks. Our code will be released soon.*

## 1. Introduction

Compositional Video Generation (CVG) focuses on generating high-quality videos from complex user prompts [25, 26, 52]. These prompts describe complex scenes with multiple interacting instances, each characterized by its own appearance and motion categories. As commercial video generation models [4, 24, 39, 42] are increasingly deployed, CVG has been widely applied in real-world scenarios, such as virtual reality [22] and human-computer interaction [62]. However, a crucial challenge of such generation models is their inability to the diversity of motion categories. As a result, generated motions appear overly similar, even with markedly distinct user prompts.

In recent years, CVG frameworks have been widely investigated for modeling realistic motion of individual instances [19, 30, 32, 45, 57]. These frameworks typically comprise a dual-stage process. First, a large language model (LLM) serves as the video planner to generate the sequence of bounding boxes for each instance. Second, the video generator constrains the motion of instances to follow the trajectories defined by these box sequences. However, generating diverse categories of motion remains a challenge, because (1) *Motion semantics are ambiguous*. Directly generating box sequences from user prompts may cause broken motion paths and abnormal size variations, owing to linguistic ambiguity. (2) *Motion guidance is rough*. Uniform diffusion guidance fails to differentiate among diverse motion categories, leading to conflated and implausible dynamics.

In this paper, we propose a motion factorization framework to improve motion diversity, as shown in Fig. 1. Specifically, we decompose motion into three primary categories (motionlessness, rigid, and non-rigid motions), with each instance uniquely assigned to a single category. Based on this categorization, we propose two modules to sequentially plan and guide motion generation. First, to resolve motion ambiguity in user prompts, we develop a Structured Motion Reasoning (SMR) module (Sec. 3.2). Instead of directly inferring motion representations from the

prompt, our module structures the prompt into a motion graph representing instances and their interactions. This graph enables reasoning about motion laws to generate diverse spatial-temporal layouts. Second, we design a Disentangled Motion Guidance (DMG) module (Sec. 3.3) that synthesizes diverse motion through specialized guidance branches. Static instances are anchored to a reference frame to maintain consistent appearance and position. For rigidly moving instances, we enforce geometric invariance leveraging a frame-agnostic shape template. Under non-rigid motion, flexible shape variation of each instance is modeled with a dense pixelwise displacement field.

To evaluate the performance of our framework on CVG, we construct datasets that cover more complex and diverse scenarios. The prompts in our dataset are derived from descriptions of real-world videos rather than handcrafted templates. We implement our framework on both VideoCrafter-v2.0 [8] (3D U-Net architecture) and CogVideoX-2B [54] (DiT architecture), and validate its effectiveness on these datasets. Comprehensive experiments demonstrate the superiority of our approach on CVG, particularly in generating desired motion categories for each instance.

Our contributions can be summarized as follows:

- We enhance motion diversity in CVG by factorizing scene dynamics into three canonical categories, including motionlessness, rigid, and non-rigid motions.
- To yield unambiguous motion representations, we introduce a structured motion graph as a bridge to reason about motion laws across diverse motion categories.
- To enable disentangled synthesis, we design specialized guidance branches for appearance consistency, geometric invariance, and local deformation.
- Through extensive experiments, we show that our framework achieves superior motion generation performance across both 3D U-Net and DiT architectures.

## 2. Related Works

**Compositional Visual Generation.** To model multiple instances and relationships in complex scenes, compositional visual generation has been explored. For image, some approaches [9, 12, 29] parse compositional semantic units from complex prompts. Others [38, 49, 50] progressively update noisy embeddings during the sampling process to align with compositional bounding boxes. For video, semantics and location across time-axis should be also considered. In semantic understanding, VideoTetris [45] decomposes prompts at both frame and instance levels. Vico [53] rebalances token importance of action-related words. In sampling guidance, LVD [30] and VideoDirectorGPT [32] use sequences of bounding boxes to capture instance displacements. However, such approaches fail to consider the diversity of motion categories, often generating overly similar motion across diverse instances.

**LLMs-Assisted Video Generation.** LLMs have made a significant impact in natural language processing due to their ability to understand open-world knowledge [36, 59]. Some recent studies [15, 17, 18, 30, 32, 33, 37, 61] have utilized LLMs to assist video generation by parsing user prompts as additional guidance. For example, Direct2V [17] and FreeBloom [18] divide user prompts into separate prompts for each frame, enabling the generation of time-varying scenes. FlowZero [33] and DyST-XL [15] synthesize bounding boxes to guide the dynamic interactions between multiple objects. Vlogger [61] elaborates a user story into a script to achieve long video generation. However, the above frameworks still face challenges in reasoning about the diverse interactions among multiple instances. This is mainly because they lack structured modeling to handle the semantic ambiguity of prompts.

**Motion Guidance in Video Generation.** Given the crucial role of motion in video generation, some studies have endeavored to synthesize realistic dynamics by leveraging diverse motion signals. Pioneering works such as VMC [21], LAMP [48], DrugNUWA [55] and OnlyFlow [23] focus on replicating motion categories in reference videos. But, such imitation fails to generalize to unseen motion types. In recent years, some researchers have explored motion guidance based on user-provided sparse or dense motion fields [3, 31, 34, 34, 40, 58]. TrailBlazer [34] and FreeTraj [40] regard bounding boxes annotated in keyframes as a sparse motion field, providing rough movement direction of a few pixels. The motionPrompting [13] expands user-provided mouse drags into more complex semi-dense motion flows. However, these approaches generally adopt the uniform motion guidance paradigm, failing to account for the motion diversity of individual instances within a scene.

### 3. Methodology

#### 3.1. Overall Framework

Our framework assigns heterogeneous motion prototypes (ranging from motionlessness to rigid and non-rigid motions) to distinct instances, conditioned on their motion categories. This framework is organized into cascaded modules following *planning before generation* paradigm. Specifically, in Sec. 3.2, we propose an Structured Motion Reasoning (SMR) module, which represents motion categories as position and scale variations across bounding box sequences, inferred from the structured motion graph. Bounding box sequences collectively form the spatial-temporal layout.

$$\{\mathcal{B}_1, \mathcal{B}_2, \dots, \mathcal{B}_F\} = \text{LLM}(\mathcal{R}; C) \quad (1)$$

where  $\{\mathcal{B}_1, \mathcal{B}_2, \dots, \mathcal{B}_F\}$  denotes the spatial-temporal layout.  $\mathcal{R}$  specifies the structured motion graph,  $C$  is the user-provided prompts.  $F$  is the frame number.

Conditioned on these layouts, in Sec. 3.3, we present a Disentangled Motion Guidance (DMG) module, which enables diverse motion synthesis through separate constraints on appearance consistency, geometric invariance, and spatial deformation. These branches transform spatial-temporal layout into the motion-specific masks to optimize attention maps. This process consequently updates the video embeddings  $\mathbf{z}_{1:F}^t$ . In practice, for 3D U-net architecture, we gradually update  $\mathbf{z}_{1:F}^t$  by:

$$\mathbf{z}_{1:F}^{t-1} \leftarrow \mathbf{z}_{1:F}^t - \nabla \mathcal{L}, \quad (2)$$

$$\mathcal{L} = 1 - \frac{\beta}{P} \sum (\mathbf{A} \odot (\mathcal{G}_m + \mathcal{G}_r + \mathcal{G}_{nr})), \quad (3)$$

where  $\mathbf{A}$  denotes the attention map.  $P$  is the number of pixels.  $\beta$  denotes the guidance factor.  $\mathcal{G}_m$ ,  $\mathcal{G}_r$ , and  $\mathcal{G}_{nr}$  are masks designed to guide the generation of motionless, rigidly moving, and non-rigidly moving instances. For the DiT architecture, we directly modify the original scores:

$$\mathbf{A} = \text{Softmax} \left( \frac{\mathbf{QK}^\top (1 + \beta \odot (\mathcal{G}_m + \mathcal{G}_r + \mathcal{G}_{nr}))}{\sqrt{d}} \right). \quad (4)$$

The preliminaries are described in Appendix A.

#### 3.2. Structured Motion Reasoning

This module aims to infer motion representations that capture both individual behaviors and pairwise interactions by leveraging the semantic reasoning capability of LLMs, as shown in Fig. 2. However, user-provided prompts are often semantically ambiguous, which renders direct motion inference from such prompts unreliable. To address semantic ambiguity, we convert the original prompts into a structured motion graph, organizing instances with their associated actions and pairwise relationships. Conditioned on each instance’s motion label, we infer its bounding box sequences from motion cues derived from the motion graph. These box sequences form motion representations, encoding diverse motion categories through position and scale variations across frames.

**Motion Graph Construction.** To capture motion semantics of individual instances, we construct the motion graph through parsing compositional prompts. Specifically, each described instance is represented as a node in the graph, annotated with its corresponding motion attributes and a canonical motion label. The motion attributes are parsed by identifying verbs or predicate phrases linked to each instance. When such predicates are absent, attributes are inferred from the context. Determined by analyzing the motion attributes and instance category, each node is assigned a canonical motion label. Directed edges encode pairwise relationships between instances, including spatial relationships (e.g., “next to”, “on top of”) and dynamic interactions (e.g., “pass by”, “move toward”). Formally, we denote this

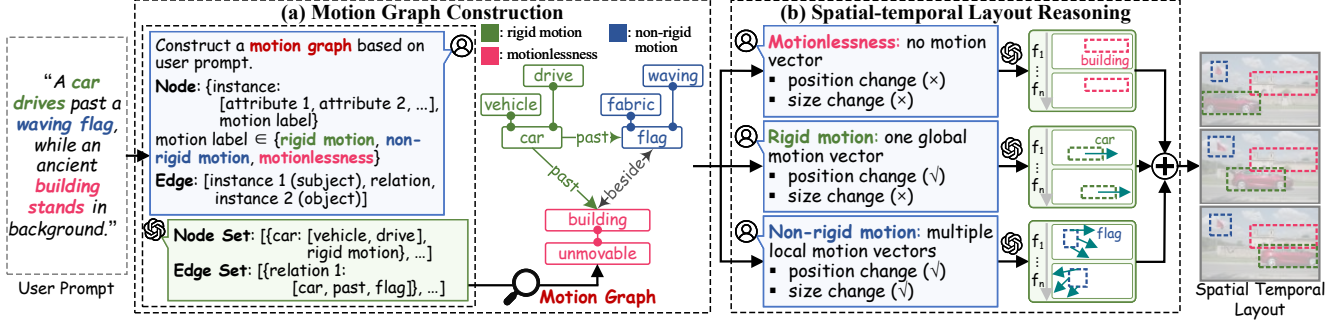


Figure 2. Overview of our Structured Motion Reasoning (SMR) module ( Sec. 3.2). (a) Given a user prompt, we organize it into a motion graph describing instances and their interactions. (b) For each instance, conditioned on its motion category, we infer a bounding box sequence from graph-derived motion cues. All bounding box sequences are then composed into a coherent spatial-temporal layout.

graph as  $\mathcal{R} = (\mathcal{V}, \mathcal{E})$ , where  $\mathcal{V}$  and  $\mathcal{E}$  respectively represent the nodes and directed edges described above.

**Spatial-temporal Layout Reasoning.** We generate motion representations for diverse categories by leveraging semantic cues encoded in constructed motion graph. Let  $v_n \in \mathcal{V}$  denote the unique identifier of the  $n$ -th instance, and  $\mathcal{B}_f(v_n)$  signify the bounding box in the  $f$ -th frame. For *motionless instances*, the position and size of the bounding box remain unchanged across all frames; that is,  $\mathcal{B}_f(v_n) = \mathcal{B}_1(v_n)$  for all  $f$ . For *rigidly moving instance*, the position of the bounding box is updated at the current frame based on the estimated velocity  $\vec{u}_{v_n}$  and acceleration  $\vec{a}_{v_n}$ .

$$\mathcal{B}_f(v_n) = \mathcal{B}_{f-1}(v_n) + \vec{u}_{v_n} + \frac{1}{2}\vec{a}_{v_n}, \quad (5)$$

where  $\vec{v}_{v_n}$  and  $\vec{a}_{v_n}$  are predicted from the previous movement of the bounding box within a sliding window, guided by action cues in the motion graph. Unlike rigid motion that applies a single displacement vector to the entire instance, *non-rigid motion* is modeled by multiple directional cues affecting distinct regions. In view of this, we infer boundary-wise displacement vectors  $\Delta_f(v_n)$  by using the localized deformation implicitly captured in the motion graph. These vectors are used to update the bounding box by considering asymmetric shifts along its boundary:

$$\mathcal{B}_f(v_n) = \mathcal{B}_{f-1}(v_n) + \Delta_f(v_n). \quad (6)$$

### 3.3. Disentangled Motion Guidance

This module aims to enhance motion diversity during the synthesis process of video diffusion model by separately modulating motion categories of each instance. As shown in Fig. 3, unlike previous approaches which adopt uniform guidance across diverse motion types [34, 40], we design *reference conditioned guidance* to enhance cross-frame appearance consistency of motionless instances; *geometric invariance guidance* to preserve geometric invariance

of rigidly moving instances; *spatial deformation guidance* to capture complex deformations of instances undergoing non-rigid movements.

**Reference Conditioned Guidance.** Video diffusion models often induce spurious variations in static regions, causing undesired flicker between frames. To preserve cross-frame appearance consistency, we anchor pixel-wise features in motionless regions to a stable reference frame. Specifically, we identify a reference frame  $f^*$  using the minimum inter-frame feature difference criterion, under the assumption that a static instance has minimal appearance variation over time.

$$f^* = \arg \min_f \sum_{f'=1}^F D(\varphi(\mathbf{z}_f^t), \varphi(\mathbf{z}_{f'}^t)), \quad (7)$$

where  $D(\cdot, \cdot)$  denotes the feature distance metric. Afterward, we achieve pixel-to-pixel appearance consistency by aligning features of all the frames to the reference frame through a masking strategy. The mask is defined as:

$$\mathcal{G}_m[x, y, f, f'](v_n) = \mathbb{1}(f' = f^* \& (x, y) \in \mathcal{B}(v_n)), \quad (8)$$

where  $\mathbb{1}(\cdot)$  denotes the indicator function, which returns 1 if the condition holds and 0 otherwise.

**Geometric Invariance Guidance.** When geometric constraints are absent, video generative models often distort rigid instances, yielding misaligned shapes. To preserve geometric invariance of rigid bodies, we confine cross-frame interactions to geometrically aligned regions derived from a frame-agnostic shape template. Specifically, we apply  $k$ -means clustering to separate background regions from bounding boxes, yielding foreground masks with clear shape contours. Unfortunately, such masks contain segmentation noise, leading to misaligned shapes. Given this, we aggregate coarse masks through a pixelwise consensus to generate a shape template. This template is inversely warped to each frame, producing geometrically aligned

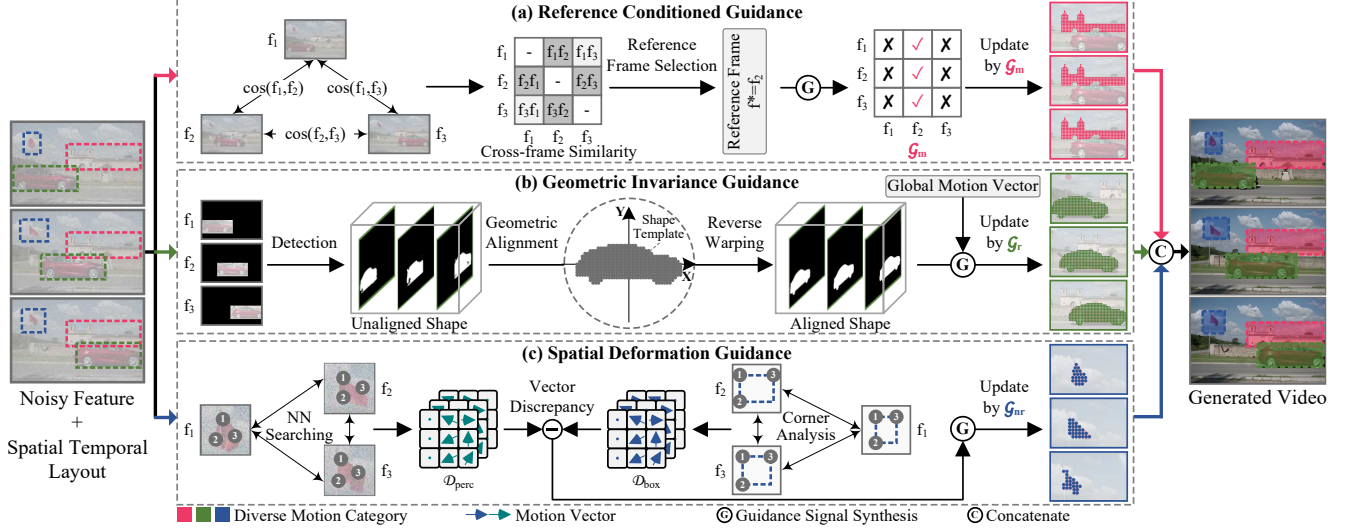


Figure 3. Overview of Disentangled Motion Guidance (DMG) module ( Sec. 3.3). (a) For motionless instances, we enforce each frame interacts only with a designated anchor frame. (b) For rigidly moving instances, we restrict cross-frame interactions of a foreground within the shape aligned regions. (c) For instances undergoing non-rigid movements, we minimize pixel-wise discrepancies between perceptual deformations and box-induced deformations.

foreground masks.

$$\mathcal{M}_f(v_n) = \text{Warp}\left(\text{Thr}\{\text{k-means}(\mathcal{B}_{f'}(v_n))\}_{f'=1}^F\right), \quad (9)$$

where  $\text{Thr}(\cdot)$  denotes the operation of pixelwise voting. In addition, we modulate the intensity of feature interactions using the displacement magnitude between frames. This is measured by the Euclidean distance between the bounding box centers of any two frames:

$$\Gamma[f, f'] = \exp(-\alpha \cdot \|\mathbf{C}_f - \mathbf{C}_{f'}\|_2) + 1, \quad (10)$$

where  $\Gamma[f, f']$  represents the displacement penalty factor between frame  $f$  and  $f'$ .  $\alpha > 0$  is a scaling factor.  $\mathbf{C}_f$  and  $\mathbf{C}_{f'}$  are center coordinates of the bounding box  $\mathcal{B}_f(v_n)$  and  $\mathcal{B}_{f'}(v_n)$ , respectively. Given both  $\Gamma$  and  $\mathcal{M}_f(v_n)$ , mask values are computed as follows:

$$\mathcal{G}_r(v_n) = \mathcal{M}(v_n) \cdot \mathcal{M}(v_n)^\top \odot \Gamma. \quad (11)$$

**Spatial Deformation Guidance.** Non-rigid motion involves complex deformations, with each pixel exhibiting diverse velocities and directions. To regularize deformation of instances undergoing non-rigid motion, we minimize pixel-level discrepancies between perceptual deformations from diffusion features and box-induced deformations. Specifically, we use pixel-wise nearest neighbor search across frames to obtain perceptual deformations  $\mathcal{D}_{\text{perc}}$ . Our key insight is that cross-frame deformation can be regarded as a many-to-many pixel correspondence problem. And pixel correspondences in RGB space are approx-

imately preserved in diffusion features [14].

$$\mathcal{N}(i, j) = \arg \min_{(i', j')} \left\| \varphi(\mathbf{z}_f^t)_{i, j} - \varphi(\mathbf{z}_{f'}^t)_{i', j'} \right\|_2, \quad (12)$$

$$\mathcal{D}_{\text{perc}}[i, j] = \mathcal{N}(i, j) - (i, j), \quad (13)$$

where  $\mathcal{N}(i, j)$  denotes the matched position of pixel  $(i, j)$ . Thereafter, we obtain box-induced deformations  $\mathcal{D}_{\text{box}}$  by computing the displacement of box corners as basic motion vectors and propagating them to all positions inside the box through bilinear interpolation.

$$\mathcal{D}_{\text{box}}[i, j] = \text{Interp}(\{\mathbf{d}_k\}_{k=1}^4, (i, j)), \quad (14)$$

where  $\mathbf{d}_k$  denotes the displacement of the  $k$ -th box corner, and  $\text{Interp}(\cdot)$  specifies bilinear interpolation operation. Based on the differences between  $\mathcal{D}_{\text{perc}}$  and  $\mathcal{D}_{\text{box}}$ , we modulate cross-frame correlation to follow desired non-rigid deformation as follows:

$$\Lambda[i, j] = \exp(-\alpha \cdot (\mathcal{D}_{\text{perc}}[i, j] - \mathcal{D}_{\text{box}}[i, j])) + 1, \quad (15)$$

$$\mathcal{G}_{\text{nr}} = (\mathcal{M}(v_n) \cdot \mathcal{M}(v_n)^\top) \odot \Lambda, \quad (16)$$

where  $\mathcal{M}(v_n)$  denotes the foreground masks obtain by  $k$ -means clustering.  $\Lambda[i, j]$  represents the deformation penalty factor of the position  $(i, j)$ .

## 4. Experiments

### 4.1. Experimental Setups

**Benchmarks.** We construct new benchmarks for CVG performance evaluation, by selecting compositional video descriptions from real-world video datasets MSR-VTT [51]

Table 1. Performance comparison of cross-modal compositional video generation approaches on our CVGBench-m and CVGBench-p datasets. Best/2nd best scores are **bolded/underlined**. † indicates compositional generation models.

Models	CVGBench-m					CVGBench-p				
	Subject Consistency	Background Consistency	Temporal Flickering	Motion Smoothness	Dynamic Degree	Subject Consistency	Background Consistency	Temporal Flickering	Motion Smoothness	Dynamic Degree
LVDM [16]	88.74%	91.27%	89.37%	91.76%	84.55%	91.05%	92.60%	91.26%	93.79%	68.78%
modelScope [46]	93.17%	93.93%	94.69%	96.23%	51.82%	95.71%	95.28%	96.01%	97.27%	30.81%
ZeroScope [1]	96.41%	95.69%	97.40%	98.66%	30.77%	97.40%	96.24%	97.73%	98.84%	16.10%
LATTE [35]	90.91%	94.33%	92.79%	94.78%	77.44%	95.21%	96.11%	95.42%	97.02%	51.66%
VideoCrafter-v1.0 [7]	97.06%	96.59%	96.04%	97.27%	38.16%	84.97%	92.51%	80.99%	83.02%	80.26%
Show-1 [56]	95.39%	95.44%	97.37%	98.23%	31.85%	97.50%	96.47%	98.41%	98.93%	11.45%
LaVie [47]	93.22%	94.36%	93.73%	96.17%	78.90%	95.45%	95.67%	95.73%	97.38%	57.40%
VideoCrafter-v2.0 [8]	97.68%	97.28%	96.28%	98.16%	33.11%	<u>98.30%</u>	<u>97.62%</u>	97.00%	98.48%	18.22%
+ BoxDiff† [50]	97.42%	96.93%	96.33%	98.25%	38.31%	98.08%	97.32%	96.87%	98.50%	25.44%
+ R&B† [49]	97.37%	96.87%	96.47%	98.21%	38.35%	98.11%	97.30%	96.83%	98.56%	25.45%
+ A&R† [38]	97.48%	97.05%	96.43%	98.27%	38.40%	97.90%	97.10%	96.83%	98.47%	31.44%
+ Vico† [53]	<u>97.72%</u>	<u>97.43%</u>	<u>96.68%</u>	<u>98.35%</u>	<u>40.00%</u>	98.23%	97.36%	<u>97.10%</u>	<u>98.56%</u>	<u>32.85%</u>
+ Ours	<b>98.40%</b>	<b>98.11%</b>	<b>97.39%</b>	<b>98.63%</b>	<b>82.21%</b>	<b>98.81%</b>	<b>98.29%</b>	<b>97.82%</b>	<b>98.79%</b>	<b>78.24%</b>
CogVideoX-2B [54]	<u>91.33%</u>	<u>92.78%</u>	95.01%	96.88%	87.80%	92.85%	93.32%	96.11%	97.95%	79.85%
+ R&P† [6]	91.00%	90.85%	<u>95.07%</u>	<u>96.96%</u>	<u>91.02%</u>	<u>93.01%</u>	<u>94.26%</u>	<u>96.12%</u>	<u>97.95%</u>	<u>81.52%</u>
+ Ours	<b>98.27%</b>	<b>97.73%</b>	<b>98.25%</b>	<b>98.74%</b>	<b>96.00%</b>	<b>98.74%</b>	<b>98.23%</b>	<b>98.38%</b>	<b>98.94%</b>	<b>87.06%</b>

and Panda-70M [10]. To consider linguistic diversity, we categorize descriptions into four compositional modes: Coordinating Structure, Quantitative Expression, Collective Noun, and Interactive Verb, as detailed in Appendix B. Guided by such categorization, we employ Llama-v3.3-70B [2] to identify samples with the above linguistic modes. As a result, we obtain two benchmarks: CVGBench-m (1665 samples from MSR-VTT) and CVGBench-p (994 samples from Panda-70M).

**Evaluation metrics.** We adopt five “Temporal Quality” metrics, as defined in VBench [20]: (1) Subject Consistency: measures consistency of a foreground instance’s appearance by computing the similarity of DINO features [5]; (2) Background Consistency: assesses coherence of the background scene by calculating the similarity of CLIP features [41]; (3) Temporal Flickering: is computed as the mean absolute difference between consecutive frames; (4) Motion Smoothness: evaluates continuity of generated motions based on motion priors from AMT model [28]; and (5) Dynamic Degree: uses RAFT model [44] to assess whether a generated video has large motions.

**Baselines.** We compare our approach against several groups of open-source baseline models: (1) Traditional T2V models. These include LVDM [16], modelScope [46], LATTE [35], LaVie [47], Show-1 [56], VideoCrafter-v1.0 [7], VideoCrafter-v2.0 [8], OpenSora-v1.2 [60], T2V-Turbo-v2.0 [27], and CogVideoX-2B [54]; (2) Compositional T2V model. This includes VideoTetris [45] and Vico [53]; (3) Compositional T2I model. We use VideoCrafter-v2.0 as the baseline to reproduce BoxDiff [50], R&B [49], and A&R [38]. Similarly, we use CogVideoX-2B as the

baseline to reproduce R&P [6].

**Implementation details.** For *structured motion reasoning* module, we use LLaMA-v3.3-70B [11] as a baseline model. For *disentangled motion guidance* module, we apply this to both VideoCrafter-v2.0 [8] and CogVideoX-2B [54]. VideoCrafter-v2.0 adopts Unet design, while CogVideoX-2B utilizes DiT architecture. Since motion guidance requires avoiding instance omission as a prerequisite, we incorporate A&R [38] and R&P [6] into VideoCrafter-v2.0 and into CogVideo-2B, respectively. The hyperparameters are set as follows: for VideoCrafter-v2.0, we set the guidance factor  $\beta$  to 10 and apply motion guidance during denoising steps 1 to 25; for CogVideoX-2B,  $\beta$  is set to 0.15 and the guidance is applied during steps 1 to 10.

## 4.2. Quantitative Comparisons

As shown in Tab. 1, we perform a comprehensive evaluation of various video generation models. In both VideoCrafter-v2.0 [8] (3D U-Net architecture) and CogVideoX-2B [54] (DiT architecture) baselines, our framework achieves steady improvements across all five evaluation dimensions on the CVGBench-m and CVGBench-p benchmarks. For example, compared to the compositional visual generation approach R&P [6], our framework can improve Subject Consistency from 91.00% to 98.27%, Background Consistency from 90.85% to 97.73%, Temporal Flickering from 95.07% to 98.25%, Motion Smoothness from 96.96% to 98.74%, and Dynamic Degree from 91.02% to 96.00%. However, R&P sometimes compromises Subject and Background Consistency. This is because R&P is designed to solve semantic leakage between instances in a frame-independent



Figure 4. Visualization comparisons under diverse motion categories, including motionlessness (top row), rigid motion (middle row), and non-rigid motion (bottom row). In 3D Unet architecture, we compare our framework with baseline VideoCrafter-v2.0 [8] and compositional approach A&R [38]. While in DiT architecture, we compare our framework with baseline CogVideoX-2B [54] and compositional approach R&P [6]. Our framework yields improved cross-frame consistency and motion fidelity across various scenarios.

manner, but neglects to model the cross-frame consistency. Our framework is able to rectify motion categories in an instance independent manner. For static instances, pixel-wise consistency across frames is enforced; for moving ones, displacement follows predefined motion vectors.

Additional quantitative evaluation on the T2V benchmark [43] are described in [Appendix C](#).

### 4.3. Qualitative Comparisons

As shown in Fig. 4, we provide visualization comparisons on generating diverse motion categories, including motionlessness, rigid motion, and non-rigid motion. Considering motionless scenarios (e.g., “static container”, or “man and woman standing”), our approach effectively suppresses

undesired movement. This arises from our approach’s capability to be aware of cross-frame feature consistency. Considering rigid motion examples (e.g., “ambulance driving”, or “riding a golf cart”), our method can not only preserve global instance integrity but also enforce displacement. Other methods suffer from unnatural deformation or minimal motion. This stems from our method’s ability to enforce geometric invariance as instances move. Considering non-rigid motion cases (e.g., “people dancing”, or “boxer fighting”), our framework produces more expressive body dynamics, while comparison methods fail to preserve coherent pose progression. This is because our framework can effectively model complex deformation by pixel-wise motion fields.

Table 2. Ablation analysis of diverse paradigms of motion reasoning module. Best scores are **bolded**.

Models	Subject Consistency	Background Consistency	Temporal Flickering	Motion Smoothness	Dynamic Degree
Baseline: VideoCrafter-v2.0 [8]					
Ours	<b>98.40%</b>	<b>98.11%</b>	<b>97.39%</b>	<b>98.63%</b>	82.21%
w/o SMR	83.90%	90.89%	83.89%	85.46%	<b>94.71%</b>
Baseline: CogVideoX-2B [54]					
Ours	<b>98.27%</b>	<b>97.73%</b>	<b>98.25%</b>	<b>98.74%</b>	<b>96.00%</b>
w/o SMR	93.16%	93.76%	95.98%	97.51%	88.21%

Table 3. Ablation analysis of diverse backbones for motion reasoning. Best scores are **bolded**.

Backbones	Subject Consistency	Background Consistency	Temporal Flickering	Motion Smoothness	Dynamic Degree
Baseline: VideoCrafter-v2.0 [8]					
LLaMA-8B [11]	97.55%	97.35%	96.55%	98.22%	75.34%
LLaMA-70B [2]	<b>98.40%</b>	<b>98.11%</b>	<b>97.39%</b>	<b>98.63%</b>	<b>82.21%</b>
Baseline: CogVideoX-2B [54]					
LLaMA-8B [11]	96.70%	96.34%	97.32%	98.17%	94.77%
LLaMA-70B [2]	<b>98.27%</b>	<b>97.73%</b>	<b>98.25%</b>	<b>98.74%</b>	<b>96.00%</b>

#### 4.4. Ablation Study

**Analysis of structured motion reasoning.** As shown in Tab. 2, we validate the effectiveness of our structured motion reasoning paradigm by replacing it with a direct text-to-motion pipeline. Our design brings notable improvements across all metrics, *e.g.*, Subject Consistency (93.16%→98.27%), Background Consistency (93.76%→97.73%), Temporal Flickering (95.98%→98.25%), Motion Smoothness (97.51%→98.74%), and Dynamic Degree (88.21%→96.00%). This gain is mainly because motion reasoning based on the motion graph effectively resolves semantic ambiguities.

**Analysis of large language model scale.** To assess the impact of LLM scale on the generation of scene configuration, we compare the LLaMA-3.1-8B [11] and LLaMA-3.3-70B [2] backbones. As shown in Tab. 3, the 70B model significantly outperforms the 8B counterpart, especially on Subject Consistency (97.55%→98.40%), Background Consistency (97.35%→98.11%), and Dynamic Degree (75.34%→82.21%). These highlight the superiority of stronger language model to reason frame-wise shapes and positions for each individual instance, ultimately improving video generation quality.

**Analysis of diverse guidance branches.** As shown in Tab. 4, progressively incorporating each guidance branch consistently improves all evaluation metrics. These gains arise from two factors. On one hand, all guidance enhances cross-frame feature propagation within foreground regions. For example, when using CogVideoX-2B [54] as baseline, our framework achieves a ~5.0% improvement in terms of cross-frame consistency. On the other hand, rigid and non-

Table 4. Ablation analysis of diverse motion guidance components, including Reference Conditioned Guidance (RCG), Geometric Invariance Guidance (GIG), Spatial Deformation Guidance (SDG). Best scores are **bolded**.

RCG	GIG	SDG	Subject Consistency	Background Consistency	Temporal Flickering	Motion Smoothness	Dynamic Degree
Baseline: VideoCrafter-v2.0 [8]							
×	×	×	97.48%	97.05%	96.43%	98.27%	38.40%
✓	×	×	98.11%	97.85%	97.21%	98.55%	51.60%
×	✓	×	98.07%	97.80%	97.15%	98.52%	53.60%
×	×	✓	97.71%	97.40%	96.72%	98.36%	74.85%
✓	✓	×	98.15%	97.91%	97.23%	98.57%	54.40%
✓	✓	✓	<b>98.40%</b>	<b>98.11%</b>	<b>97.39%</b>	<b>98.63%</b>	<b>82.21%</b>
Baseline: CogVideoX-2B [54]							
×	×	×	91.00%	90.85%	95.07%	96.96%	91.02%
✓	×	×	95.98%	96.03%	96.89%	97.90%	92.16%
×	✓	×	96.21%	96.07%	96.88%	97.88%	92.77%
×	×	✓	96.13%	96.14%	96.83%	97.81%	93.57%
✓	✓	×	97.19%	96.91%	97.49%	98.26%	94.56%
✓	✓	✓	<b>98.27%</b>	<b>97.73%</b>	<b>98.25%</b>	<b>98.74%</b>	<b>96.00%</b>

rigid motion guidance branches enforce video generation model to synthesize large-scale motion specified by motion representations. For instance, with VideoCrafter-v2.0 [8] as baseline, our non-rigid motion guidance yields Dynamic Degree gain of 27.81%.

Additional ablation studies are presented in Appendix D.

#### 4.5. Failure Cases

While our framework can improve motion diversity in video generation, challenges remain in handling rare semantic and emotional cues. As shown in Fig. 5a, our framework fails to generate the unusual concept “Dendroid”, likely due to its absence in the feature space of the baseline model. As shown in Fig. 5b, generated videos lack clear facial expressions to convey emotion “sad”, because of video generation models may ignore emotion cues (adjectives or adverbs) in user prompts. One promising direction to address such challenges is to use reference images which can provide concrete priors of semantic and emotion.

### 5. Conclusion

This paper proposes a motion factorization framework, enhancing motion diversity in compositional video generation without additional learning. The key idea is to decompose complex scene dynamics into diverse categories, including motionlessness, rigid motion, non-rigid motion. Thus, each motion category can be independently modeled and guided. Specifically, we *resolve semantic ambiguities* by reformulating user-provided prompts as a motion graph of instances and their interactions. This enables reliable reasoning over motion representations of individual instances. Then, we *address motion homogenization* by separately stabilizing background appearance, preserving rigid-body geometry, and regularizing non-rigid deformation. Experiments demonstrate the effectiveness of our framework in generating desired motion behaviors. Future

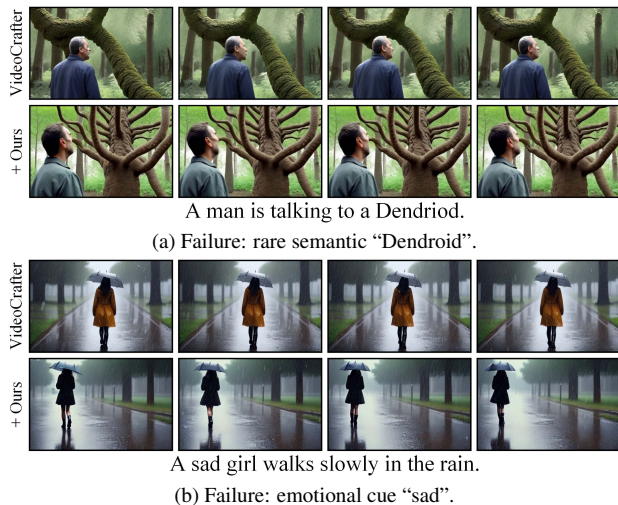


Figure 5. Baseline model and our framework can hardly generate (a) rare semantic, and (b) emotional cues.

work will explore camera poses to model global viewpoint changes across scenes.

## References

- [1] Zeroscope. 2023. 6
- [2] Llama 3.3. 2024. 6, 8
- [3] Ryan Burgert, Yuancheng Xu, Wenqi Xian, Oliver Pilarski, Pascal Clausen, Mingming He, Li Ma, Yitong Deng, Lingxiao Li, Mohsen Mousavi, et al. Go-with-the-flow: Motion-controllable video diffusion models using real-time warped noise. In *Proceedings of the IEEE/CVF Conference on Computer Vision and Pattern Recognition (CVPR)*, pages 13–23, 2025. 3
- [4] Capcut. Dreamina. <https://dreamina.capcut.com/ai-tool/home>, 2024. 2
- [5] Mathilde Caron, Hugo Touvron, Ishan Misra, Hervé Jégou, Julien Mairal, Piotr Bojanowski, and Armand Joulin. Emerging properties in self-supervised vision transformers. In *Proceedings of the IEEE/CVF International Conference on Computer Vision (ICCV)*, pages 9650–9660, 2021. 6
- [6] Anthony Chen, Jianjin Xu, Wenzhao Zheng, Gaole Dai, Yida Wang, Renrui Zhang, Haofan Wang, and Shanghang Zhang. Training-free regional prompting for diffusion transformers. *arXiv preprint arXiv:2411.02395*, 2024. 6, 7
- [7] Haoxin Chen, Menghan Xia, Yingqing He, Yong Zhang, Xiaodong Cun, Shaoshu Yang, Jinbo Xing, Yaofang Liu, Qifeng Chen, Xintao Wang, et al. Videocrafter1: Open diffusion models for high-quality video generation. *arXiv preprint arXiv:2310.19512*, 2023. 6
- [8] Haoxin Chen, Yong Zhang, Xiaodong Cun, Menghan Xia, Xintao Wang, Chao Weng, and Ying Shan. Videocrafter2: Overcoming data limitations for high-quality video diffusion models. In *Proceedings of the IEEE/CVF Conference on Computer Vision and Pattern Recognition (CVPR)*, pages 7310–7320, 2024. 2, 6, 7, 8
- [9] Junsong Chen, Chongjian Ge, Enze Xie, Yue Wu, Lewei Yao, Xiaoze Ren, Zhongdao Wang, Ping Luo, Huchuan Lu, and Zhenguo Li. Pixart- $\sigma$ : Weak-to-strong training of diffusion transformer for 4k text-to-image generation. In *European Conference on Computer Vision (ECCV)*, pages 74–91. Springer, 2024. 2
- [10] Tsai-Shien Chen, Aliaksandr Siarohin, Willi Menapace, Ekaterina Deyneka, Hsiang-wei Chao, Byung Eun Jeon, Yuwei Fang, Hsin-Ying Lee, Jian Ren, Ming-Hsuan Yang, et al. Panda-70m: Captioning 70m videos with multiple cross-modality teachers. In *Proceedings of the IEEE/CVF Conference on Computer Vision and Pattern Recognition (CVPR)*, pages 13320–13331, 2024. 6
- [11] Abhimanyu Dubey, Abhinav Jauhri, Abhinav Pandey, Abhishek Kadian, Ahmad Al-Dahle, Aiesha Letman, Akhil Mathur, Alan Schelten, Amy Yang, Angela Fan, et al. The llama 3 herd of models. *arXiv e-prints*, pages arXiv–2407, 2024. 6, 8
- [12] Patrick Esser, Sumith Kulal, Andreas Blattmann, Rahim Entezari, Jonas Müller, Harry Saini, Yam Levi, Dominik Lorenz, Axel Sauer, Frederic Boesel, et al. Scaling rectified flow transformers for high-resolution image synthesis. In *International Conference on Machine Learning (ICML)*, 2024. 2
- [13] Daniel Geng, Charles Herrmann, Junhwa Hur, Forrester Cole, Serena Zhang, Tobias Pfaff, Tatiana Lopez-Guevara, Yusuf Aytar, Michael Rubinstein, Chen Sun, et al. Motion prompting: Controlling video generation with motion trajectories. In *Proceedings of the IEEE/CVF Conference on Computer Vision and Pattern Recognition (CVPR)*, pages 1–12, 2025. 3
- [14] Michal Geyer, Omer Bar-Tal, Shai Bagon, and Tali Dekel. Tokenflow: Consistent diffusion features for consistent video editing. *arXiv preprint arXiv:2307.10373*, 2023. 5
- [15] Weijie He, Mushui Liu, Yunlong Yu, Zhao Wang, and Chao Wu. Dyst-xl: Dynamic layout planning and content control for compositional text-to-video generation. *arXiv preprint arXiv:2504.15032*, 2025. 3
- [16] Yingqing He, Tianyu Yang, Yong Zhang, Ying Shan, and Qifeng Chen. Latent video diffusion models for high-fidelity long video generation. *arXiv preprint arXiv:2211.13221*, 2022. 6
- [17] Susung Hong, Junyoung Seo, Heeseong Shin, Sunghwan Hong, and Seungryong Kim. Direct2v: Large language models are frame-level directors for zero-shot text-to-video generation. *arXiv preprint arXiv:2305.14330*, 2023. 3
- [18] Hanzhuo Huang, Yufan Feng, Cheng Shi, Lan Xu, Jingyi Yu, and Sibe Yang. Free-bloom: Zero-shot text-to-video generator with llm director and ldm animator. *Advances in Neural Information Processing Systems (NeurIPS)*, 36:26135–26158, 2023. 3
- [19] Kaiyi Huang, Yukun Huang, Xuefei Ning, Zinan Lin, Yu Wang, and Xihui Liu. Genmac: compositional text-to-video generation with multi-agent collaboration. *arXiv preprint arXiv:2412.04440*, 2024. 2
- [20] Ziqi Huang, Yinan He, Jiashuo Yu, Fan Zhang, Chenyang Si, Yuming Jiang, Yuanhan Zhang, Tianxing Wu, Qingyang Jin,

- Nattapol Chanpaisit, et al. Vbench: Comprehensive benchmark suite for video generative models. In *Proceedings of the IEEE/CVF Conference on Computer Vision and Pattern Recognition (CVPR)*, pages 21807–21818, 2024. 6
- [21] Hyeonho Jeong, Geon Yeong Park, and Jong Chul Ye. Vmc: Video motion customization using temporal attention adaptation for text-to-video diffusion models. In *Proceedings of the IEEE/CVF Conference on Computer Vision and Pattern Recognition (CVPR)*, pages 9212–9221, 2024. 3
- [22] Yize Jin, Meixu Chen, Todd Goodall, Anjul Patney, and Alan C Bovik. Subjective and objective quality assessment of 2d and 3d foveated video compression in virtual reality. *IEEE Transactions on Image Processing (IEEE TIP)*, 30: 5905–5919, 2021. 2
- [23] Mathis Koroglu, Hugo Caselles-Dupré, Guillaume Jeanerret, and Matthieu Cord. Onlyflow: Optical flow based motion conditioning for video diffusion models. In *Proceedings of the IEEE/CVF Conference on Computer Vision and Pattern Recognition (CVPR)*, pages 6226–6236, 2025. 3
- [24] Kuaishou. Kling. <https://kling.kuaishou.com/>, 2024. 2
- [25] Wentao Lei, Jinting Wang, Fengji Ma, Guanjie Huang, and Li Liu. A comprehensive survey on human video generation: Challenges, methods, and insights. *arXiv preprint arXiv:2407.08428*, 2024. 2
- [26] Chengxuan Li, Di Huang, Zeyu Lu, Yang Xiao, Qingqi Pei, and Lei Bai. A survey on long video generation: Challenges, methods, and prospects. *arXiv preprint arXiv:2403.16407*, 2024. 2
- [27] Jiachen Li, Qian Long, Jian Zheng, Xiaofeng Gao, Robinson Piramuthu, Wenhui Chen, and William Yang Wang. T2v-turbo-v2: Enhancing video generation model post-training through data, reward, and conditional guidance design. *arXiv preprint arXiv:2410.05677*, 2024. 6
- [28] Zhen Li, Zuo-Liang Zhu, Ling-Hao Han, Qibin Hou, Chun-Le Guo, and Ming-Ming Cheng. Amt: All-pairs multi-field transforms for efficient frame interpolation. In *Proceedings of the IEEE/CVF Conference on Computer Vision and Pattern Recognition (CVPR)*, pages 9801–9810, 2023. 6
- [29] Zhimin Li, Jianwei Zhang, Qin Lin, Jiangfeng Xiong, Yanxin Long, Xincheng Deng, Yingfang Zhang, Xingchao Liu, Minbin Huang, Zedong Xiao, et al. Hunyuan-dit: A powerful multi-resolution diffusion transformer with fine-grained chinese understanding. *arXiv preprint arXiv:2405.08748*, 2024. 2
- [30] Long Lian, Baifeng Shi, Adam Yala, Trevor Darrell, and Boyi Li. Llm-grounded video diffusion models. In *International Conference on Learning Representations (ICLR)*, 2024. 2, 3
- [31] Jingyun Liang, Yuchen Fan, Kai Zhang, Radu Timofte, Luc Van Gool, and Rakesh Ranjan. Movidio: Motion-aware video generation with diffusion model. In *European Conference on Computer Vision (ECCV)*, pages 56–74. Springer, 2024. 3
- [32] Han Lin, Abhay Zala, Jaemin Cho, and Mohit Bansal. Videodirectorgpt: Consistent multi-scene video generation via llm-guided planning. *Conference on Language Modeling (CoLM)*, 2024. 2, 3
- [33] Yu Lu, Linchao Zhu, Hehe Fan, and Yi Yang. Flowzero: Zero-shot text-to-video synthesis with llm-driven dynamic scene syntax. *arXiv preprint arXiv:2311.15813*, 2023. 3
- [34] Wan-Duo Kurt Ma, JP Lewis, and W Bastiaan Kleijn. Trailblazer: Trajectory control for diffusion-based video generation. *arXiv preprint arXiv:2401.00896*, 2023. 3, 4
- [35] Xin Ma, Yaohui Wang, Gengyun Jia, Xinyuan Chen, Ziwei Liu, Yuan-Fang Li, Cunjian Chen, and Yu Qiao. Latte: Latent diffusion transformer for video generation. *arXiv preprint arXiv:2401.03048*, 2024. 6
- [36] Shervin Minaee, Tomas Mikolov, Narjes Nikzad, Meysam Chenaghlu, Richard Socher, Xavier Amatriain, and Jianfeng Gao. Large language models: A survey. *arXiv preprint arXiv:2402.06196*, 2024. 3
- [37] Gyeongrok Oh, Jaehwan Jeong, Sieun Kim, Wonmin Byeon, Jinkyu Kim, Sungwoong Kim, and Sangpil Kim. Mevg: Multi-event video generation with text-to-video models. In *European Conference on Computer Vision (ECCV)*, pages 401–418. Springer, 2024. 3
- [38] Quynh Phung, Songwei Ge, and Jia-Bin Huang. Grounded text-to-image synthesis with attention refocusing. In *Proceedings of the IEEE/CVF Conference on Computer Vision and Pattern Recognition (CVPR)*, pages 7932–7942, 2024. 2, 6, 7
- [39] Pika. Pika. <https://www.pika.art>, 2024. 2
- [40] Haonan Qiu, Zhaoxi Chen, Zhouxia Wang, Yingqing He, Menghan Xia, and Ziwei Liu. Freetraj: Tuning-free trajectory control in video diffusion models. *arXiv preprint arXiv:2406.16863*, 2024. 3, 4
- [41] Alec Radford, Jong Wook Kim, Chris Hallacy, Aditya Ramesh, Gabriel Goh, Sandhini Agarwal, Girish Sastry, Amanda Askell, Pamela Mishkin, Jack Clark, et al. Learning transferable visual models from natural language supervision. In *International Conference on Machine Learning (ICML)*, pages 8748–8763. PmlR, 2021. 6
- [42] Runway. Introducing gen-3 alpha: A new frontier for video generation. <https://runwayml.com/research/introducing-gen-3-alpha>, 2024. 2
- [43] Kaiyue Sun, Kaiyi Huang, Xian Liu, Yue Wu, Zihan Xu, Zhenguo Li, and Xihui Liu. T2v-compbench: A comprehensive benchmark for compositional text-to-video generation. In *Proceedings of the IEEE/CVF Conference on Computer Vision and Pattern Recognition (CVPR)*, pages 8406–8416, 2025. 7
- [44] Zachary Teed and Jia Deng. Raft: Recurrent all-pairs field transforms for optical flow. In *European Conference on Computer Vision (ECCV)*, pages 402–419. Springer, 2020. 6
- [45] Ye Tian, Ling Yang, Haotian Yang, Yuan Gao, Yufan Deng, Xintao Wang, Zhaochen Yu, Xin Tao, Pengfei Wan, Di ZHANG, et al. Videotetris: Towards compositional text-to-video generation. In *Advances in Neural Information Processing Systems (NeurIPS)*, pages 29489–29513, 2024. 2, 6
- [46] Jiuniu Wang, Hangjie Yuan, Dayou Chen, Yingya Zhang, Xiang Wang, and Shiwei Zhang. Modelscope text-to-video technical report. *arXiv preprint arXiv:2308.06571*, 2023. 6

- [47] Yaohui Wang, Xinyuan Chen, Xin Ma, Shangchen Zhou, Ziqi Huang, Yi Wang, Ceyuan Yang, Yinan He, Jiashuo Yu, Peiqing Yang, et al. Lavie: High-quality video generation with cascaded latent diffusion models. *International Journal of Computer Vision (IJCV)*, pages 1–20, 2024. 6
- [48] Ruiqi Wu, Liangyu Chen, Tong Yang, Chunle Guo, Chongyi Li, and Xiangyu Zhang. Lamp: Learn a motion pattern for few-shot video generation. In *Proceedings of the IEEE/CVF Conference on Computer Vision and Pattern Recognition (CVPR)*, pages 7089–7098, 2024. 3
- [49] Jiayu Xiao, Henglei Lv, Liang Li, Shuhui Wang, and Qingming Huang. R&b: Region and boundary aware zero-shot grounded text-to-image generation. *arXiv preprint arXiv:2310.08872*, 2023. 2, 6
- [50] Jinheng Xie, Yuexiang Li, Yawen Huang, Haozhe Liu, Wentian Zhang, Yefeng Zheng, and Mike Zheng Shou. Boxdiff: Text-to-image synthesis with training-free box-constrained diffusion. In *Proceedings of the IEEE/CVF International Conference on Computer Vision (ICCV)*, pages 7452–7461, 2023. 2, 6
- [51] Jun Xu, Tao Mei, Ting Yao, and Yong Rui. Msr-vtt: A large video description dataset for bridging video and language. In *Proceedings of the IEEE Conference on Computer Vision and Pattern Recognition (CVPR)*, pages 5288–5296, 2016. 5
- [52] Haiwei Xue, Xiangyang Luo, Zhanghao Hu, Xin Zhang, Xunzhi Xiang, Yuqin Dai, Jianzhuang Liu, Zhensong Zhang, Minglei Li, Jian Yang, et al. Human motion video generation: A survey. *IEEE Transactions on Pattern Analysis and Machine Intelligence (TPAMI)*, 2025. 2
- [53] Xingyi Yang and Xinchao Wang. Compositional video generation as flow equalization. *arXiv preprint arXiv:2407.06182*, 2024. 2, 6
- [54] Zhuoyi Yang, Jiayan Teng, Wendi Zheng, Ming Ding, Shiyu Huang, Jiazheng Xu, Yuanming Yang, Wenyi Hong, Xiaohan Zhang, Guanyu Feng, et al. Cogvideox: Text-to-video diffusion models with an expert transformer. *arXiv preprint arXiv:2408.06072*, 2024. 2, 6, 7, 8
- [55] Shengming Yin, Chenfei Wu, Jian Liang, Jie Shi, Houqiang Li, Gong Ming, and Nan Duan. Dragnuwa: Fine-grained control in video generation by integrating text, image, and trajectory. *arXiv preprint arXiv:2308.08089*, 2023. 3
- [56] David Junhao Zhang, Jay Zhangjie Wu, Jia-Wei Liu, Rui Zhao, Lingmin Ran, Yuchao Gu, Difei Gao, and Mike Zheng Shou. Show-1: Marrying pixel and latent diffusion models for text-to-video generation. *International Journal of Computer Vision (IJCV)*, pages 1–15, 2024. 6
- [57] Hongyu Zhang, Yufan Deng, Shenghai Yuan, Peng Jin, Zesen Cheng, Yian Zhao, Chang Liu, and Jie Chen. Magiccomp: Training-free dual-phase refinement for compositional video generation. *arXiv preprint arXiv:2503.14428*, 2025. 2
- [58] Zhenghao Zhang, Junchao Liao, Menghao Li, Zuozhuo Dai, Bingxue Qiu, Siyu Zhu, Long Qin, and Weizhi Wang. Tora: Trajectory-oriented diffusion transformer for video generation. In *Proceedings of the IEEE/CVF Conference on Computer Vision and Pattern Recognition (CVPR)*, pages 2063–2073, 2025. 3
- [59] Wayne Xin Zhao, Kun Zhou, Junyi Li, Tianyi Tang, Xiaolei Wang, Yupeng Hou, Yingqian Min, Beichen Zhang, Junjie Zhang, Zican Dong, et al. A survey of large language models. *arXiv preprint arXiv:2303.18223*, 2023. 3
- [60] Zangwei Zheng, Xiangyu Peng, Tianji Yang, Chenhui Shen, Shenggui Li, Hongxin Liu, Yukun Zhou, Tianyi Li, and Yang You. Open-sora: Democratizing efficient video production for all. *arXiv preprint arXiv:2412.20404*, 2024. 6
- [61] Shaobin Zhuang, Kunchang Li, Xinyuan Chen, Yaohui Wang, Ziwei Liu, Yu Qiao, and Yali Wang. Vlogger: Make your dream a vlog. In *Proceedings of the IEEE/CVF Conference on Computer Vision and Pattern Recognition (CVPR)*, pages 8806–8817, 2024. 3
- [62] Ran Zuo, Xiaoming Deng, Keqi Chen, Zhengming Zhang, Yu-Kun Lai, Fang Liu, Cuixia Ma, Hao Wang, Yong-Jin Liu, and Hongan Wang. Fine-grained video retrieval with scene sketches. *IEEE Transactions on Image Processing (IEEE TIP)*, 32:3136–3149, 2023. 2